Aerosol Science and Technology, 44:612–628, 2010

ISSN: 0278-6826 print / 1521-7388 online
DOI: 10.1080/02786826.2010.481298

The Detection Efficiency of the Single Particle Soot Photometer

J. P. Schwarz,[1,2] J. R. Spackman,[1,2] R. S. Gao,[1] A. E. Perring,[1,2] E. Cross,[3] T. B. Onasch,[3] A. Ahern,[4] W. Wrobel,[4] P. Davidovits,[4] J. Olfert,[5] M. K. Dubey,[6] C. Mazzoleni,[7] and D. W. Fahey[1,2]

[1] *Chemical Sciences Division, Earth System Research Laboratory, National Oceanic and Atmospheric Administration, Boulder, Colorado, USA*
[2] *Cooperative Institute for Research in Environmental Sciences, University of Colorado, Boulder, Colorado USA*
[3] *Aerodyne Research, Inc., Billerica, Massachusetts, USA*
[4] *Department of Chemistry, Boston College, Chestnut Hill, Massachusetts, USA*
[5] *University of Alberta, Mechanical Engineering Building, Edmonton, Alberta, Canada*
[6] *Los Alamos National Laboratory, Los Alamos, New Mexico, USA*
[7] *Michigan Technological University, Houghton, Michigan, USA*

A single particle soot photometer (SP2) uses an intense laser to heat individual aerosol particles of refractory black carbon (rBC) to vaporization, causing them to emit detectable amounts of thermal radiation that are used to quantify rBC mass. This approach is well suited for the detection of the majority of rBC mass loading in the ambient atmosphere, which occurs primarily in the accumulation mode (∼1–300 fg-rBC/particle). In addition to operator choices about instrument parameters, SP2 detection of rBC number and/or mass can be limited by the physical process inherent in the SP2 detection technique — namely at small rBC mass or low laser intensities, particles fail to heat to vaporization, a requirement for proper detection. In this study, the SP2's ability to correctly detect and count individual flame-generated soot particles was measured at different laser intensities for different rBC particle masses. The flame-generated soot aerosol used for testing was optionally prepared with coatings of organic and non-organic material and/or thermally denuded. These data are used to identify a minimum laser intensity for accurate detection at sea level of total rBC mass in the accumulation mode (300 nW/(220-nm PSL)), a minimum rBC mass (∼0.7-fg rBC-mass corresponding to 90 nm volume-equivalent diameter) for near-unity number detection efficiency with a typical operating laser intensity (450 nW/(220-nm PSL)), and a methodology using observed color temperature to recognize laser intensity insufficient for accurate rBC mass detection. Additionally, methods for measurement of laser intensity using either laboratory or ambient aerosol are presented.

Received 30 September 2009; accepted 21 March 2010.
NOAA SP2 participation was supported by the NOAA Atmospheric Composition and Climate, and Health of the Atmosphere Programs, and the NASA Radiation Sciences Program and Upper Atmosphere Research Program. The intercomparison was supported in part by the Office of Science (BER), Department of Energy (Atmospheric Science Program) grant No. DE-FG02-05ER63995, and the Atmospheric Chemistry Program of the National Science Foundation, grant No. ATM-0525355.
Address correspondence to Joshua Schwarz, 325 Broadway R/CSD-6, Boulder, CO 80305. USA. E-mail: Joshua.p.schwarz@noaa.gov

1. INTRODUCTION

Refractory black carbon (rBC) aerosol is the most important particulate absorber of solar radiation in the atmosphere. Its direct contribution to the radiation budget of the globe is only exceeded by CO_2 and methane (Forster et al. 2007). Due to its non-uniform spatial distribution, rBC induces more dramatic regional forcing than either CO_2 or methane (e.g., Tripathi et al. 2005). In addition to direct aerosol absorption aloft, rBC is suspected to significantly impact climate through indirect (as cloud-condensation nuclei (e.g., Zuberi et al. 2005)), semi-direct (dehydration of clouds (e.g., Lohmann and Feichter, 2001)), and snow albedo (increased snow melt (e.g., Flanner et al. 2007)) effects.

Traditionally, rBC has been a difficult species to measure with sufficient specificity and sensitivity. Although it is responsible for most of the aerosol absorption in the visible wavelength range, it is typically only a small contributor to total aerosol mass and extinction. The fact that rBC is non-soluble and refractory (i.e., vaporizing only at very high temperature) means that traditionally effective techniques used to quantify sulfate, salt, and organic aerosols are generally insensitive to rBC. Aerosol optical absorption has long been used as a proxy for rBC mass, but as it can be influenced by both non-rBC aerosol absorbers (e.g., dust or brown carbon), and by the enhancement of rBC

absorption by coatings (which evolve in time) (e.g., Schnaiter et al. 2005), absorption measurements alone do not form a robust approach to quantifying ambient loadings of rBC.

The Single Particle Soot Photometer (SP2, Droplet Measurement Technologies, Inc., Boulder, CO) has become increasingly recognized as a valuable tool for quantifying aerosol rBC. There are several ways in which the SP2 provides previously unavailable information. First, it unambiguously measures the mass of rBC in individual aerosol particles rather than inferring bulk rBC loadings from measurements of aerosol optical/absorption properties. Second, the SP2 is able to determine the mixing state of individual rBC-containing particles and provide some information about the amount of non-refractory material associated with an rBC component. Third, as the instrument detects individual aerosol particles, it is able to quantify rBC loadings even in clean conditions where other techniques would require prohibitively long integration times. Detection of individual particles also allows straightforward testing of the instrument.

Since the first applications of the SP2 for *in situ* measurements, its response to particle mass, composition, morphology, and coating state have been tested in laboratory settings (Schwarz et al. 2006; Slowik et al. 2007; Moteki and Kondo 2007, Cross et al. 2009). These tests indicate that over a defined mass range the thermal radiation emitted by a rBC particle at its vaporization temperature is linearly proportional to its mass and independent of the morphology or mixing state of the particle. As a result, the rBC mass of individual particles has been used to construct accumulation-mode size distributions between 1–300 fg rBC mass (corresponding to ∼100 and ∼650 nm volume-equivalent diameter (VED), assuming void-free rBC with a density of 2 g/cm^3). This size range generally contains most (∼90%) of the accumulation-mode rBC mass for typical ambient conditions (Schwarz et al. 2008b; Shiraiwa et al. 2008). The inferred number distribution of ambient rBC tends to peak at or below 1 fg rBC mass (100 nm VED) in urban emissions (Schwarz et al. 2008a), and below this size for fresh emissions, for example, from aircraft (Petzold and Schröder 1998).

At present the lower rBC mass limit of detection of the SP2 is determined by the laser intensity necessary to heat rBC particles to vaporization, a requirement for the particles to be correctly detected. Laser heating of rBC particles in the SP2 is a separate process from that of detection of the thermal emissions. Although either aspect of measurement can affect the SP2s ability to properly quantify rBC masses or detect rBC number, this paper is focused primarily on the laser/rBC interaction. One would expect, a priori, that smaller (spherical) particles are harder to heat to vaporization than larger (spherical) particles because their absorption of laser power scales as the particle volume, yet convective heating of the surrounding air (the main energy loss term of a hot rBC particle) scales as particle surface area (Stephens et al. 2003; Moteki and Kondo 2007). In fact, although rBC particles are not spherical, at low laser intensity (or at low mass) they fail to heat sufficiently to reach their vaporization temperature and thus to emit thermal radiation at the level characteristic of rBC mass at vaporization. In these situations the SP2 fails to correctly detect all of the rBC particles that it samples.

A great deal of both experimental and theoretical work (Schulz et al. 2006) has been done in the field of pulsed laser-induced incandescence (LII), which shares many detection and interpretation issues with the SP2. Pulsed LII techniques rely on interrogating bulk aerosol with repeated pulses of high-intensity laser light, and then recording the evolution in time of the resulting thermal radiation from the aerosol. Laser power is transferred to the aerosol only during the duration of each pulse ($< \sim$20 ns). The questions addressed in this paper (in the context of the SP2) deal with a very different situation: the SP2 CW laser intensity is less than the peak intensity of individual LII pulses and is used to heat only individual particles over much longer time scales ($> \sim 10$ μs). Hence, unfortunately, understanding of pulsed LII is not immediately relevant to practical issues of SP2 rBC detection.

SP2 detection of rBC number below 3.5 fg rBC mass (150 nm VED) has not yet been adequately addressed. Here we present measurements of SP2 detection of rBC number as a function of rBC mass per particle, SP2 laser intensity and rBC mixing state. This work was done within the framework of a laboratory intercomparison of the SP2 with other instruments sampling flame-generated soot in July 2008 (Cross et al. 2009). The intercomparison expands upon an earlier study (Slowik et al. 2007). The soot aerosol was optionally prepared with coatings of organic and non-organic material and/or thermally denuded before being sampled with the instruments. The configuration of the SP2 with other instrumentation relevant to this paper is shown in Figure 1.

The flame-generated soot aerosols tested here are used as a proxy to evaluate SP2 detection of ambient rBC. The data are used to define a practical lower limit to the rBC mass-per-particle detection of the SP2 technique and identify a minimum laser intensity threshold for use in SP2 measurements of rBC mass loadings in typical conditions at sea level. This paper also includes methods for the absolute measurement of laser intensity, a protocol for identification of laser intensities that are too low for correct rBC mass detection, a discussion of the appropriate signal parameters to use in analyzing SP2 data, and discussion about the meaning of the term "refractory black carbon" in the context of SP2 measurements.

This paper is organized into sections describing the SP2 instrument operation and data interpretation; other critical instruments used in this work (more detailed descriptions may be found in (Cross et al, 2009)); generation of test rBC aerosol; determination of SP2 detection efficiency; experimental results from specific tests; and the conclusions from this study and recommendations for the SP2 user community. A glossary of abbreviations is included.

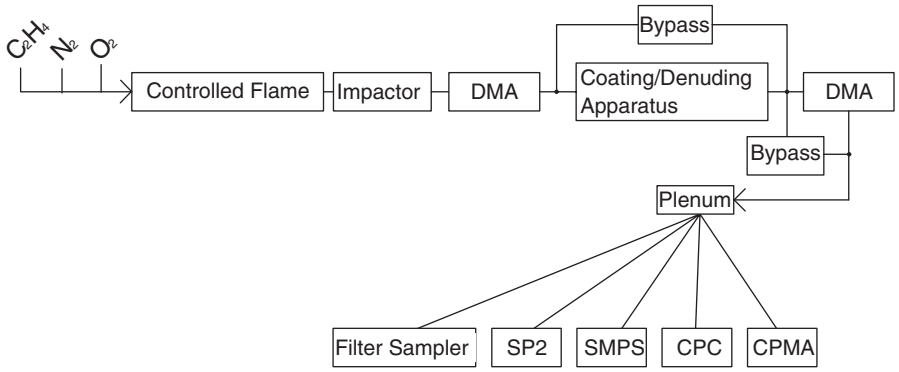

FIG. 1. Schematic of the flame-generated soot generation and detection scheme with the filter sampler, single particle soot photometer (SP2), scanning mobility particle sizer (SMPS), condensation particle counter (CPC), Couette centrifugal particle mass analyzer (CPMA), and differential mobility analyzer (DMA).

2. SP2 INSTRUMENT AND PROCEDURES

2.1. Single Particle Soot Photometer (SP2) Apparatus

The SP2 consists of an intense intra-cavity laser, a flow control system to confine sample aerosol to the center 1/4 of the laser beam, four optical detectors focused on the intersection of the sample aerosol with the laser beam, and electronic resources necessary to store the response of the detectors to individual particles crossing the laser beam (Figure 2).

A solid-state pump laser (808 nm, Unique-Mode AG, Jena, Germany) is fiber-optically coupled to a Nd:YAG crystal that is coated on one side with a reflective coating at 1064 nm. The coating defines one side of the laser cavity, while a high-reflectivity mirror defines the other side. The laser is tuned such that it is in a TEM 0,0 mode, i.e., with a Gaussian intensity profile. A pinhole aperture (I.D. 2.3 mm) is placed in the cavity to constrain the spatial mode of the laser and reduce pump light leakage into the cavity. Some laser radiation (at 1064 nm) leaks through the mirror. This light is filtered to remove contributions from the pump laser and detected with a "leakage" photodetector, providing a convenient relative measure of laser intensity. Since the amount of leakage depends on the (unknown) quality of the mirror, the photodetector signal cannot be used to derive an absolute measure of the laser intensity within the cavity. With independent calibration, however, the signal can be used as a relative measure of intensity (as in Section 2.3). Note that although the laser cavity is defined by high-reflectivity mirrors, the cavity finesse, Q, is limited by the Nd:YAG crystal itself to a low value (on order ~100). Thus the laser beam is expected to be insensitive to the small perturbation caused by the presence of a small particle in its path. This insensitivity has been confirmed through inspection of the leakage light when particles traversed the laser.

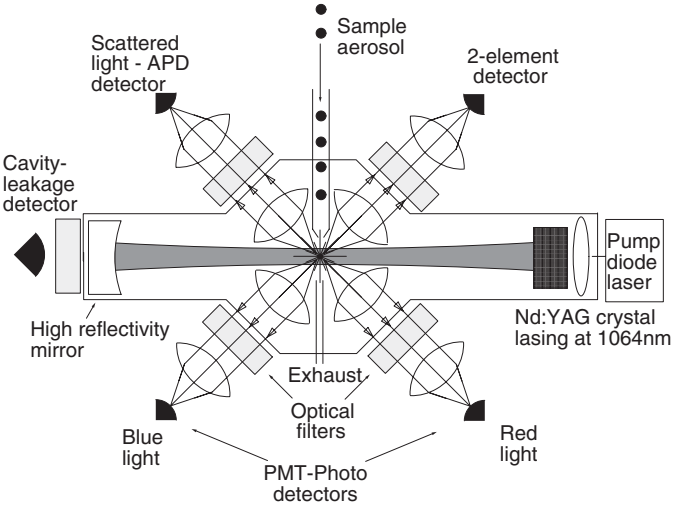

FIG. 2. Schematic of the Single Particle Soot Photometer (SP2) following Schwarz et al. (2006). The sample aerosol is confined with filtered sheath flow to the center 1/4 of the laser beam, and then drawn out of the laser cavity through the exhaust line. Although drawn in the page for simplicity, the sample line and exhaust lines extend perpendicular to the detection axes (i.e., vertically into and out of the page).

Sample aerosol is continuously introduced to the laser cavity through a capillary (typically 0.43 mm ID). The input aerosol stream is confined to the center ~ 1/4 of the laser (which has a ~1.1 mm 95% intensity width), so individual particles traversing the beam experience peak intensities of ~70–100% of the intensity at its center. The measurement of the width of the aerosol jet was made with PSL particles in the diameter range of 200–600 nm. It is possible that diffusion may increase the width of the jet for small particles ($\ll$200 nm), thereby reducing the efficiency of their detection by the SP2. Here this mechanism is not addressed. The aerosol interacts with the laser at a pressure that is typically within 20 hPa of ambient (i.e., sea-level pressure, 1013 hPa) in this study.

The aerosol flow into the SP2 is measured with a laminar flow element; the pressure difference across the element is proportional to the volume flow through the element. The laminar flow element was calibrated several times over the course of the intercomparison with a Gilian flow standard (Gilibrator 2, Sensidyne, Clearwater, FL, USA). In general, the sample flow remained constant as long as the upstream plenum pressure was

unperturbed. Changes in sample flow were easily observed. The SP2 often sampled at very low flow (∼15 vccm) in order to avoid multiple particles crossing the laser at the same time, and to extend the time that aerosol was sampled without generating excessively large data sets. In these cases electronic noise dominated the flow signal at time scales below 10 s, and necessitated averaging the flow over periods that were sometimes longer than the periods that particle data were recorded for a given laser intensity with each experimental setup.

As shown in Figure 2, the intersection of the aerosol jet and the laser is imaged onto four optical detectors. One of the detectors is an avalanche photo-detector (APD, model C30916E, Perkin-Elmer Optoelectronics, Quebec, Canada) with sensitivity at 1060 nm measured by the manufacturer (which we assume matches its sensitivity at 1064 nm). The optical path to this detector (henceforth referred to as the "scatter detector") includes an optical filter (RG850, 2 mm thick, Schott North America Inc., Elmsford, NY, USA) passing light at 1064 nm (i.e., laser light scattered by particles) and blocking visible thermal radiation and scattered pump laser light. The APD gain depends on temperature, hence we recommend operating the SP2 at temperatures within 5 C of 23 C (approximately the temperature at which the APD manufacturer specifies its gain).

Two of the detectors detect visible light from thermal emissions in either a blue or red wavelength band (henceforth referred to as the "blue channel" or the "red channel"). The ratio of the amount of thermal radiation detected in these two wavelength bands (the "color ratio") provides a color temperature measurement that constrains rBC composition (Schwarz et al. 2006). The thermal radiation emitted by a vaporizing rBC particle extends into the infrared so the scatter detector also detects some thermal radiation. However, for most rBC particles the infrared component is negligibly small compared to the true scattered light signal. For the smallest rBC detected (VED $\leq \sim$100 nm), where this would have the largest relative effect, the thermal signal typically contributes ∼10% to the scatter signal. The fourth detector, which is not used in this analysis, provides the position of each rBC particle in the laser beam during its transit, and is used to measure the optical size of an rBC-containing particle before it is significantly heated by the laser (Gao et al. 2007).

The imaging system of each channel includes two optics that first collimate the light from the particle/laser interaction and then focus it on a detector. The optics of the scatter channel (except the RG850 filter previously mentioned) are coated with an anti-reflective coating to maximize transmittance of the infrared scattered light signal to the APD. The coatings are specified to transmit >99% of the infrared light incident on them. Laboratory tests of 5 such optics indicated their transmission efficiency actually varied with a standard deviation of 5%. As there are two optics per channel, the total variability in transmission efficiency of scattered light between different SP2s is estimated to be <10%. The optics for the visible light channels are coated with an anti-reflection coating for the visible wavelengths which is much less (i.e., ∼30% less) effective in the near infrared than the infrared-specific coating.

When a particle containing rBC enters the laser beam, it absorbs energy and heats. Any non-refractory materials associated with the rBC (henceforth generically referred to as coatings) will be vaporized at relatively low temperature, and the rBC core will continue to heat until it reaches its vaporization temperature (identified in the range 3700–4300 K by Schwarz et al. (2006); and in the smaller range 4230–4325K by Moteki and Kondo (2009)). At this point, some of the power absorbed from the laser maintains the temperature difference between the vaporizing particle and the surrounding air, while the remainder contributes to the emission of thermal radiation (largely in the visible wavelength range for rBC) and to the phase change of the rBC material from a solid to a vapor (Stephens et al. 2003). Tests of rBC of ∼8 fg mass in both a helium atmosphere, and in air at various pressures, showed that the peak visible light (and its color ratio) emitted by these particles at vaporization is not pressure or atmosphere-composition dependent. This indicates that combustion processes do not contribute to the visible light signal as detected in SP2 instruments.

The NOAA SP2 uses photomultiplier tubes (PMTs) to detect the visible light in the blue and red channels. A reference voltage input controls the gain on each PMT. Calibrations over periods up to six weeks indicate that, as long as the PMTs and laser have not been perturbed (e.g., the PMT removed and replaced on the instrument, or the output mirror of the laser adjusted), the PMT gain is stable within 10%. The effective gain of a detector may be represented as the ratio of the peak voltage recorded by the computer system to the corresponding mass of rBC in the detected particle. This gain may be expressed in units of V/fg-rBC mass. Such a gain value (which may be determined by empirical measurement) reduces the complexity of the spectral emissions, detector sensitivities, and optical collection efficiencies to one variable. The NOAA SP2 typically operates with a gain of ∼0.05–0.06 V/ fg-rBC in both the blue and red visible channels, which allows excellent coverage of typical ambient rBC mass distributions in the accumulation mode. The manufacturer specifies the PMTs to be only slightly dependent on temperature in the visible wavelengths, and we expect negligible temperature dependencies in the system electronics.

We have attempted to relate color temperature at vaporization for different rBC materials to the SP2's sensitivity to their mass. These attempts have not been successful, perhaps because of the narrow range of color temperatures identified for different rBC materials by Moteki and Kondo (2009). Thus, until further testing sheds more light on this issue, a single PMT-sensitivity calibration is used for all ambient rBC.

Color ratio, as a proxy for color temperature, may be used to constrain rBC composition. Color ratio may be measured for a variety of rBC and non-rBC materials in the laboratory, and used to generate a "color map" that identifies the range of ratios associated with rBC for the specific instrumental configuration being used. If sufficient contrast in the wavelength bands

associated with the red and blue channels exists, the color ratio range associated with rBC will not overlap with that of other materials (Schwarz et al. 2006).

The color ratio measurement obtained with the NOAA SP2 relies upon using PMTs with different photocathode sensitivities. In contrast, the SP2 configuration sold by the manufacturer (Droplet Measurement Technology, Inc., Boulder, CO) uses two PMTs of the same type (H6779-0, Hamamatsu Corp., Tokyo, Japan) with color contrast achieved by filtering out the blue light (with a short-wave cutoff at 630 nm) for the red channel. In the NOAA system the blue PMT is the same type used by DMT, with sensitivity in the blue wavelength range (peak sensitivity at ~350–450 nm), while the red PMT is a model that is more sensitive in the red (model H6779-02 or model H6779-20, with peak sensitivities at wavelengths in the range of 450–650 nm). The red PMT has enough sensitivity at the pump-laser wavelength to require the use of an optical filter to remove light at wavelengths longer than ~750 nm. Additionally, an optical aperture is placed in front of the detector. An advantage of this configuration is that signal sensitivity in the red is maximized. An advantage of the traditional configuration is that the blue PMT has no sensitivity to the laser and thus requires less care in setup.

Older SP2 instruments used APD detectors with filters for the red and blue channel measurements—presently all SP2s are operated with PMTs. For APD-equipped instruments the detection of rBC particles was limited to detection of larger rBC (>~3 fg) by the lower gain of the APDs.

2.2. Refractory Black Carbon and the SP2

The variety and complexity of the microphysical state and composition of carbon-containing light absorbing aerosols, as well as the experimental difficulty in unambiguously measuring the refractory carbon component of these aerosols, have resulted in confusing terminology in the field of absorbing carbonaceous aerosols (Andreae and Gelenscér 2006). "Black carbon" is generally used in the literature to refer to a material with optical properties and composition similar to combustion-generated aggregates of spherules primarily composed of carbon, but not including the organic materials typically associated with combustion particles. "Refractory black carbon" is used here specifically to indicate an aerosol component with a color temperature (determined through the SP2 color-ratio measurement) in a range seen to be uniquely associated with laboratory black carbon samples and ambient rBC out of all tested aerosol constituents likely to be found in the ambient (Schwarz et al. 2006).

This range was identified by Schwarz et al. (2006) as 3700–4300 K, and more recently refined by Moteki and Kondo (2009) to 4230–4325 K. This definition contrasts with the use of the term "refractory" used in the field of thermal aerosol analysis, in which aerosol is sampled onto a filter and then thermally oxidized at increasing temperatures. Materials surviving to temperatures of 900 K, much lower than those reached in the SP2, are typically identified as refractory; in fact Andreae and Gelenscér (2006) show that the thermogram of humic acid has a peak at this temperature. However, the laser-induced heating in the SP2 requires an aerosol particle that absorbs strongly at 1064 nm. Humic acid (Alpha Aesar, Ward Hill, MA, USA) an organic carbon that tends (like many organics) to absorb most strongly in the blue visible wavelength range or below, does not heat detectably in the SP2. Refractory black carbon (rBC), defined as discussed above, has been shown to be representative of the refractory carbonaceous material produced in flames (Slowik et al. 2007; Cross et al. 2009), and thus is likely the same type of material identified by Pöschl (2003) as the most refractory and most strongly light absorbing carbonaceous aerosol material in the atmosphere. Note that the new results of Moteki and Kondo (2009) shed light on the relationship between rBC composition and thermal emissions in the SP2 and thus strengthen our understanding of the connection between laboratory rBC and that in the atmosphere.

2.3. Quantifying SP2 Laser Intensity in the Laboratory

It is necessary to measure and maintain the SP2 laser intensity in order to achieve reliable detection of rBC. An absolute measurement of laser intensity is achievable by measuring the scattered laser light from an aerosol standard. It is also possible to indirectly evaluate absolute SP2 laser intensity without use of an aerosol standard using the method outlined in Section 6.2.

NOAA SP2 laser intensity is measured with polystyrene latex spheres (PSLs) that are NIST-traceable size standards with a fixed index of refraction. Ideally, a PSL particle would traverse the center of the laser beam, producing a Gaussian detector signal in time (Gao et al. 2007) in which the maximum scattering signal was proportional to the maximum laser intensity. In practice a spread of maximal scattering signals is observed from PSL particles passing through different portions of the laser beam due to the imperfect confinement of the aerosol jet by the sheath flow. Hence, a typical sampling of ~3000 PSL particles is made, and the most probable signal amplitude is used as a measure of the laser's maximum intensity.

Calibration with PSLs can be used to relate laser intensities between two SP2 instruments. This is possible because the detection optical geometry does not vary between manufactured SP2s (although some uncertainty exists due to variations in the quality of optical elements used in the scatter channel (described in Section 2.1)), and because the absolute APD calibration is provided by the manufacturer. Comparison of gain between several APDs shows that their relative sensitivity is constant within 10% over 5 years; hence, we assume that their absolute response is stable in time. The APDs should be installed such that the images of particles passing through the laser beam are centered on their active surfaces, to insure that the manufacturer's gain calibration is valid. This can be accomplished by recording PSL signals with the detector in different positions and thereby

identifying the centered position. Note that scattering signals from larger particles can saturate the gain medium of the APD if their images are too sharply focused on the detector active surface.

To address the variability in the gain and detection electronics between different SP2s, we reference PSL measurements to the peak optical power they cause to scatter to the scatter detector, rather than the voltage signal (proportional to this power) recorded by the data system. The peak power incident on the APD from a PSL particle, P, can be calculated from the peak voltage produced by the scatter detector electronics and recorded by the data system:

$$P = \frac{[S \cdot (2.44_{(\mathrm{mV})})]}{[R1_{(\Omega)}]\,[G_2]\,[A_{(A/W)}]} * 10^6$$

where P is in units of nW/PSL – i.e., the maximal optical power incident on the scatter detector from a single PSL particle traversing the laser; S is the modal peak height of the PSLs sampled in units of 2.44-mV steps (the resolution of the SP2's high speed analog-to-digital converter); R_1 is the impedance of the resistor used in the current-to-voltage conversion—the first stage of gain in the SP2 APD board (Typically 51.1 kohm); G_2 is the gain of the second stage of amplification (typically in the range of 5–16) on the APD board; and A is the sensitivity of the APD (typically 12–15 A/W). Note that the sensitivity of the APD is dependent on both its operating bias voltage and its temperature. If APDs are not used within approximately $\pm\sim$5 C of the temperature specified by the manufacturer, the sensitivity of the scatter APD gain should be independently quantified. The NOAA SP2 has a long history of calibrations with 220-nm diameter PSLs. Hence the laser intensity values in this paper are based on the peak power incident on the scattered light detector when sampling these PSLs and are presented in units of nW/(220-nm PSL). The peak power scattered by other PSL sizes can be scaled from the 220-nm value by using Mie theory for scattering from spheres with an index of refraction of 1.59, integrated over the detection geometry of the SP2 for the intracavity laser as in Gao et al. (2007). Results from this calculation are given in Table 1.

Making the connection from the optical power incident on the APD due to the scattering of laser light by PSL to the absolute laser intensity within the cavity measured in System International (SI) units requires the use of scattering theory. Here Mie theory was used to calculate that at 1064 nm, a 220-nm PSL particle of refractive index (1.59,0) has a scattering cross-section of 0.00213 μm^2. Integrating the scattering phase function with the known geometry of the SP2, we find that 13% of the total light scattered out of the unpolarized, intra-cavity laser beam falls within the solid angle subtended by the optics of each SP2 detection axis. The collected light is collimated, transmitted through a RG850 filter, and then focused onto the scatter detector. With the highest laser intensity setting used here, the peak power incident on the scatter detector from a 220-nm PSL particle was 450 nW, representing 93% of the light incident on the detection optics (assuming the anti-reflective coating on the optics is perfect, and the remaining 7% is reflected or attenuated by the RG850 filter according to manufacturer data sheets). Thus, the total peak optical power scattered out of the laser beam by the spherule was 3.7 μW. It follows that the central laser intensity was 3.7μW/0.00213 μm^2 = 1.7 $\times$ 10^5 W/cm^2. Once absolute laser intensity is established (in whatever units one cares to work in), it can be used to calibrate the leakage photodetector as a relative measure of intensity. This calibration appears to be robust so long as the ambient temperature of the instrument does not change (i.e., the photodetector is fairly sensitive to temperature changes), the laser alignment is not changed, the photodetector is not moved, the pinhole aperture is not adjusted, or the fiber-optic connection to the pump diode laser is not modified. Figure 3 shows the relationship between the absolute laser intensity, measured with PSLs, and the relative intensity measured with the leakage photodetector. The relationship was stable to better than 20% over the course of the intercomparison.

TABLE 1
Peak scattered laser power incident on the SP2 detector from polystyrene latex spheres (PSLs). Values are normalized to the power from 220-nm PSL particles (refractive index = 1.59, 0).

PSL Diameter (nm)	Peak scattered power (relative units)
150	0.099
200	0.58
220	1.00
250	2.1
300	6.2
350	15.0
400	30.8
450	56.4
500	97.7
550	167
600	272

2.4. SP2 Data Acquisition and Analysis

The SP2 computer system digitizes the analog signals from the four optical detectors every 0.2 μs (i.e., at 5 MHz) and stores the result in a buffer holding 0.2 s of data. As the next 0.2 s of data are being acquired, the stored data are scanned for occasions when either of two detector signal values rise above trigger levels defined by the user. The choices of trigger-detector and level are made by the user. Trigger events are recorded by the computer. In recording such an event, a user-specified number of 0.2-μs data points before and after the trigger point are saved. When the scan is complete, the computer either waits

for the subsequent 0.2-s buffer to finish being acquired, or, if its analysis took longer than 0.2 s, begins searching the most recent 0.2 s of unprocessed data. Typically one of the triggering detectors is the scatter detector—thereby allowing recording of all aerosol particles with or without rBC content. The other triggering detector is traditionally the blue channel detector, resulting in the storage of signals associated with rBC particles, some of which do not have a large enough scattering cross section to trigger the scatter detector. Complete scanning of each 0.2 s buffer in less than or equal to 0.2s represents a 100% duty cycle for the SP2 instrument. In the analysis presented here, 1-s values of rBC particle counts were generated by averaging (five or fewer) 0.2-s values obtained over a 1-s period.

In post-processing of the SP2 event signals, two variables were extracted from the two visible light channels for the analysis performed here. First, the peak amplitude of blue channel was derived as the difference between the peak value and the baseline signal (determined as the average of 30 points measured in the absence of a particle event). Second, the ratio of the blue and red channel signals (baselines previously removed) was calculated from the time of peak emissions to the time when the visible light signals had decayed to one-half of their peak values. This ratio is nearly linearly proportional to the temperature of a particle emitting the thermal radiation (Schwarz et al. 2006). The relative gain of the red and blue channel detectors was set such that this ratio was 1 for the flame-generated rBC material at vaporization. Because of poor signal-to-noise in the measurement of the color ratio of individual particles, only probability distributions collected from measurements of many particles are interpreted here. The peak heights of the visible light channels are proportional to the rBC-mass of the particle (Slowik et al. 2007). Henceforth "peak heights" will only be used to refer to the visible light signals detected from rBC particles, and will not be used to refer to the scattered light signal from any particles.

3. ADDITIONAL INSTRUMENTATION

A prepared aerosol flow of FGS was provided to a plenum and then distributed to the SP2; a Scanning Mobility Particle Sizer (SMPS [TSI Model 3080]), which provided averaged size distributions; a condensation particle counter (CPC [TSI Model 3022A]), which provided 1-s total particle number concentration; a Couette Centrifugal Particle Mass Analyzer (CPMA (Olfert and Collings 2005)), which provided a measure of the absolute mass of monodisperse aerosol particles; and a filter sampling system that allowed post-experimental analysis of collected aerosol particles through electron microscopy.

3.1. Scanning Particle Mobility Sizer (SMPS)

An SMPS measured the mobility diameter distribution and the total particle concentration in an aerosol flow. Here, however, only the relative number concentrations of different sized aerosol modes are calculated and used. The average SMPS size distribution was obtained for each experimental dataset, which typically lasted 5 SMPS scans (i.e., 10 min). The stability of the size distributions measured within each dataset was excellent.

3.2. Centrifugal Particle Mass Analyzer (CPMA)

A Couette centrifugal particle-mass analyzer (CPMA, Olfert & Collings 2005; Olfert et al. 2006) was used to measure aerosol mass. The CPMA mass was calibrated to better than 2% with calibration-standard polystyrene-latex (PSL) spheres (Cross et al. 2009). This uncertainty represents the typical uncertainty in determining the mass of an unknown monodisperse aerosol. The uncertainty in determining the mass of the flame-generated soot samples analyzed here is small enough that we neglect it in our analysis.

4. BLACK CARBON AEROSOL GENERATION AND PREPARATION

An underlying assumption in this paper is that SP2 measurement of ambient rBC particles can be characterized using flame-generated soot as a proxy material. Although we are not able to evaluate the validity of this assumption, we note that the production of flame-generated soot, as discussed below, is similar to many combustion processes that contribute to ambient rBC loadings. Here flame-generated soot (FGS) was produced with a commercially available McKenna burner combusting ethylene (C_2H_4) with O_2 in a premixed dilution with N_2 (as in Cross et al. 2009). Different ratios of fuel-to-air were used to generate FGS with varying characteristics. The equivalence ratio, φ, is defined as the ratio of the actual fuel-to-oxidant (i.e., fuel-to-air) ratio to the ideal ethylene-fuel-to-oxygen ratio for complete combustion. Thus $\varphi = 1$ represents complete combustion. In this study φ was varied in the range 1.8 – 6.0. FGS generated with fairly low φ (<2.5) tends to be highly fractal and is composed mainly of refractory black carbon with a minor mass contribution from non-refractory organics. At higher φ, FGS particles contain increasing fractions of non-refractory organic material and tend to have less fractal morphology (Slowik et al. 2004). Analysis of filter samples and CPMA mass data indicate that FGS particles generated at higher φ (≥ 4) were not reduced to pure rBC when passed through a thermal denuder. Thus, measurements with $\varphi > 2.5$ are excluded from further analysis here.

The flow of FGS was cleansed of large particles (>1 μm) with an impactor and then mobility-diameter selected with a differential mobility analyzer (DMA) operating at a 10:1 sheath to sample ratio to provide a narrow range (i.e., a "mode") of aerosol mass for study. The unmodified FGS particles are referred to as "nascent" in contrast to "denuded" FGS particles in which non-refractory constituents were removed with a thermal denuder, or "coated" FGS particles in which additional coating material was added. Coatings of dioctyl sebacate (bis (2-ethylhexyl) sebacate), a liquid organic compound, or sulfuric acid (H_2SO_4) were added by passing the size-selected aerosol over a heated reservoir of the respective material.

A thermal denuder was used to remove non-refractory materials from FGS aerosols. The denuder consisted of a heated stainless steel tube (250 C, 56 cm in length) followed by a region of activated charcoal at room temperature. The material surviving passage through the denuder is assumed to be purely rBC. If some organic (i.e., non rBC) materials remain on the particles after denuding, they will cause the CPMA-measured mass to represent an upper limit on the rBC mass. Evidence that no appreciable organic material was associated with denuded rBC particles was supplied by an Aerosol Mass Spectrometer (Cross et al. 2009). As thicker coatings were applied, occasionally a mode of homogeneously nucleated particles, composed entirely of dioctyl sebacate or H_2SO_4, was generated either by the coating system or the denuding process. In some cases a second DMA was used to remove these particles from the sample (Figure 1).

Refractory black carbon-containing aerosol was distributed through a plenum to a suite of particle instruments. The flow system was leak tested by setting the DMA control voltage to zero and confirming aerosol-free air in the various instruments downstream. Air pressure at the intersection of the aerosol jet and the laser beam was approximately 1000 hPa throughout the study.

5. DETERMINATION OF SP2 DETECTION EFFICIENCY

The primary quantity of interest in this study is the SP2 detection efficiency (SDE), defined as the ratio of the SP2-measured concentration (number/unit volume) of particles with a given rBC to their actual concentration. In samples that contained particles of more than one rBC mass (e.g., in a DMA-selected FGS sample with multiply-charged modes), the concentration measurement is specific to a single modal mass. In general, the separation of modal responses in both the SP2 (i.e., in rBC mass) and the SMPS (i.e., in mobility diameter) was excellent, as shown in Figure 4. The SP2 concentration measurement of the primary mode of rBC aerosol (the mass-range of rBC with the highest concentration) was conducted as follows. A range of rBC mass (or equivalently peak height) associated with a single mode was identified, as illustrated in Figure 4. The number of rBC particles within this range of the primary mode (Figure 4) was counted over each second by the SP2. This value was corrected for the computer duty cycle based on the number of 0.2 s buffers read in that second, and then divided by the average sample flow into the SP2.

The absolute concentration of rBC particles was calculated as the CPC-measured concentration of all particles scaled by the SMPS-determined number fraction of the primary mode particles to all the particles. This approach ensured that differences in SP2 detection efficiency for multiply-charged particles with larger rBC-mass did not influence the detection efficiency determined for the primary mode of rBC particles. In a few cases, a nucleation mode of particles (non-rBC particles) dominated total particle number measured by the CPC. These cases were removed from consideration unless the SMPS was able to completely characterize the nucleation mode peak and thus the relative number concentration of the primary rBC mode.

SP2 detection efficiency depends, in general, on the mass of the detected rBC particle as well as laser intensity, visible-light detector gain, and trigger level. If detector gain is not high enough, or trigger level low enough, the signals associated with a small rBC particle will not be recorded by the SP2 computer, thus inadvertently lowering SDE. This is an issue that can be evaluated based on straightforward determination of the detector gain and choice of trigger level. For the NOAA SP2 during this study, the blue channel detector gain was increased to a sufficiently high value ($\sim$2.5 V/(fg-rBC mass)) that gain and trigger issues did not affect the measurement of SP2 detection efficiency. This gain, which is extremely high, would in theory allow detection of rBC particles as small as $\sim$0.02 fg ($\sim$30 nm VED) if they emitted thermal radiation with the same mass efficiency as observed for larger rBC particles.

The time delays between the SP2 sampling of the aerosol and the CPC sampling (due to different sample line lengths from the plenum (Figure 1), sample flow, etc.) were accounted for by comparison of the time-resolved SP2 concentrations with the CPC values, as in Figure 5 (where the time offset has been removed). Time offsets were identified to 1 s precision. Uncertainty in the time-offsets between SP2 sampling and CPC sampling do not systematically bias the calculation of SDE.

SDE was measured at different laser intensities. The laser intensity was varied over at least five values for each test aerosol sampled in the intercomparison by choosing pump-laser current values for use throughout the intercomparison. It was varied from the highest intensity possible with the existing laser alignment down to a factor 2.5 less. The maximum was roughly one-half the maximum intensity that has ever been achieved with the NOAA SP2 (900 nW/(220-nm PSL)), and was fairly typical of the SP2 laser intensity during research flights in 2004 – 2008 (Schwarz et al. 2006; Schwarz et al. 2008b). Figure 6 shows the relationship between the pump laser current and the resulting signal from the laser-cavity leakage photodetector. The relationship was stable enough ($\pm$7%) to allow using the set points to repeatedly select different laser intensity levels over the course of the measurements. This relationship is unique for each set-up of an SP2 laser.

Note that insufficient laser power for proper detection can lead to decreased thermal emissions from rBC particles because they are not heated to vaporization (as discussed in Section 6.1). However, in this case rBC particles will still be counted as "detected" so long as the resulting (incorrect) rBC mass determination is within the range associated with the primary mode. Hence, SDE as calculated here is purely representative of number-based detection efficiency.

6. EXPERIMENTAL RESULTS

Over the course of the intercomparison more than 850 measurement datasets of rBC aerosol with different masses, coating

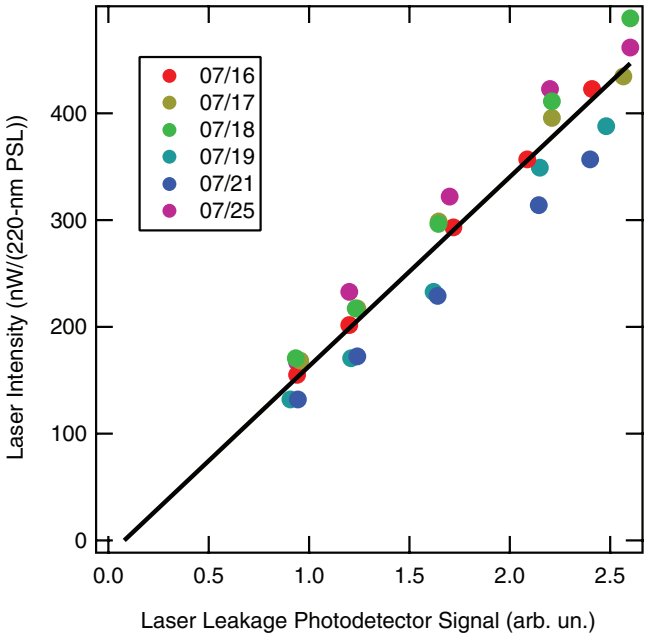

FIG. 3. Comparison of the measurement of laser intensity based on measurements inside and outside the cavity. The latter is measured with the laser leakage photodetector. The former is measured as the most probable peak power incident on the SP2 scatter detector when a polystyrene latex sphere (PSL) of known diameter and index of refraction is sampled (see text). The power in the laser cavity was varied by changing the amount of pump laser light incident on the Nd:YAG crystal.

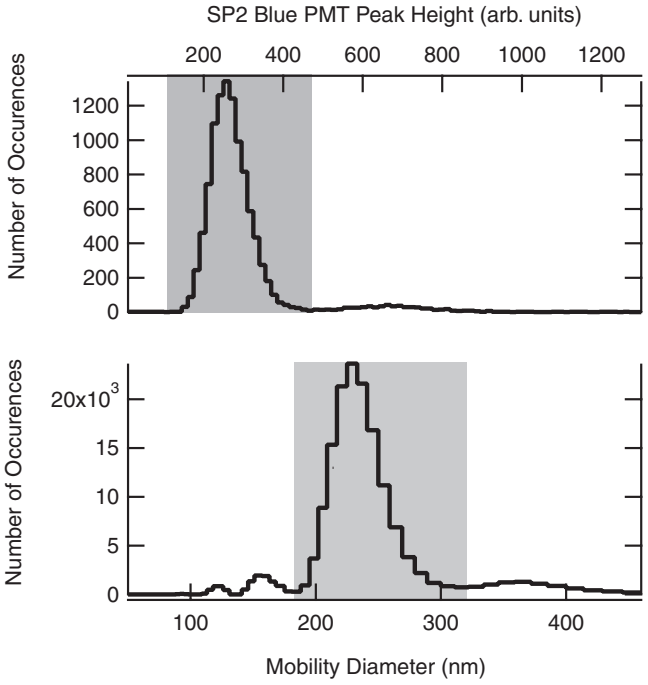

FIG. 4. Top: SP2 peak height distribution for typical sample of FGS aerosol used to in the analysis here. Bottom: the SMPS distribution for the same FGS sample. The shaded sections represent the selected peak height and diameter ranges, respectively, for the primary aerosol mode for which SP2 detection efficiency was calculated.

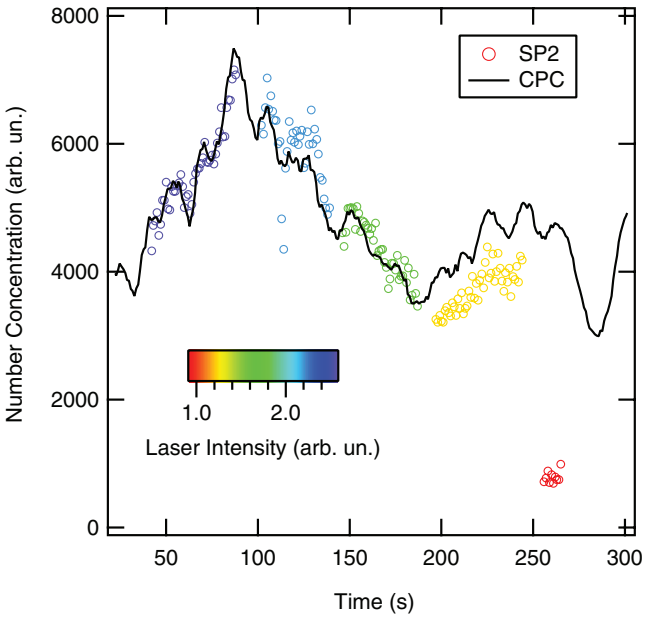

FIG. 5. Comparison of the number concentration as measured with the SP2 and the CPC sampling the same FSG aerosol during an experimental dataset. A time delay occurs between the SP2 and CPC sampling due to different sample line lengths and other differences. The time delay, identified by matching their time resolved concentrations, has already been included here so there is no apparent time offset. FSG number concentrations during a series of measurements typically varied approximately at the level shown here or somewhat less. The color scale indicates SP2 laser intensity—at low intensity detection efficiency decreases.

states, SP2 laser intensity, and equivalence ratio were made. Not all were used in this study. If a set of measurements with a single rBC core mass lacked a measurement of the denuded aerosol, the set of measurements was excluded from this analysis. A denuded measurement was necessary for the CPMA to determine the rBC mass without being influenced by contributions from non-refractory materials. The measurements used here are summarized in Table 2.

The primary question addressed in this paper can be posed as follows: for a given SP2 laser intensity and a particle of known rBC-mass and mixing state, what is the probability that upon sampling by the SP2, the rBC component will be heated to

TABLE 2
The range of values of various experimental parameters explored in this study. Aerosol generated from 94 unique configurations of these parameters was sampled at five different SP2 laser intensities

Equivalence ratio (φ)	1.8–2.5
Mobility diameter	50–300 nm
rBC mass	0.05–4 fg
Coating/rBC mass ratio	0–25
Laser intensity	160–450 nW/(220-nm PSL)

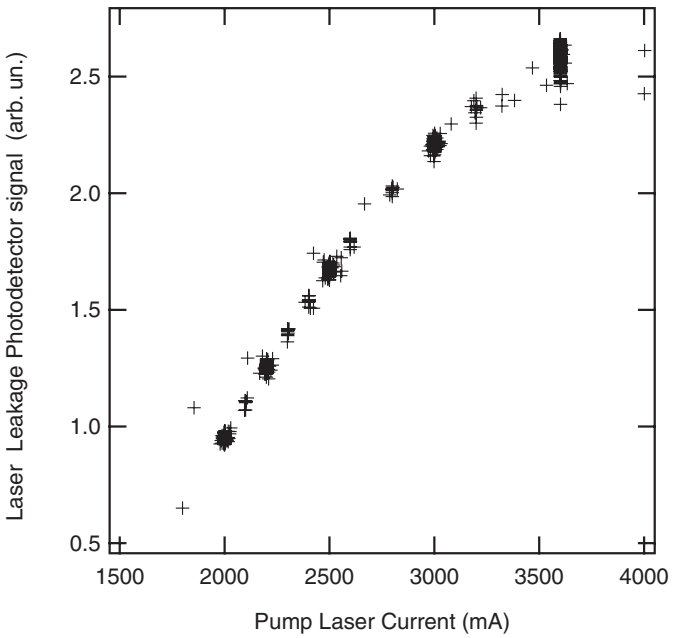

FIG. 6. Laser-cavity leakage as measured with a photodetector as a function of the current driven through the solid-state pump laser. Each data point is the value averaged over a single experimental setup and laser intensity tested (∼850 points).

vaporization and detected? In this section this primary question is explored one parameter at a time: first laser intensity, then rBC mass, and finally mixing state.

6.1. Dependence of Color Ratio, rBC Mass Determination, and Detection Efficiency on Laser Intensity

Examination of the distributions of color temperature as a function of laser intensity show that above a threshold intensity, color temperature is independent of laser intensity as all rBC particles are brought to their vaporization temperature. Below the threshold, however, the color temperatures tend to shift to lower values because some (or all) rBC particles only reach lower temperatures. Thus, color ratio eventually plateaus with increasing laser intensity. This behavior is implied in Figure 7a, for 2 fg rBC particles from FGS. The Stefan-Boltzmann law indicates that the quantity of blackbody radiation emitted from an object is proportional to its absolute temperature to the fourth power. Hence one would expect, a priori, that rBC particles will emit less visible light when below their vaporization temperature. This expectation is fully borne out; the corresponding histograms of thermal-radiation peak heights (Figure 8) clearly shift to lower values at the lower laser intensities. As heating rBC to its vaporization temperature is a requirement for proper detection, we henceforth referred to this threshold intensity as the "threshold intensity for proper detection" (TIPD). The TIPD depends on the mass, morphology, and composition of the rBC particles under test, and the composition and pressure of the surrounding air (which affects convective heat loss from the particle, as discussed above). Note that the TIPD determined for 1 fg rBC particles, for example, is higher than the TIPD for 5 fg rBC particles. The TIPD can be determined for a sample aerosol by identifying the point at which color ratio stops

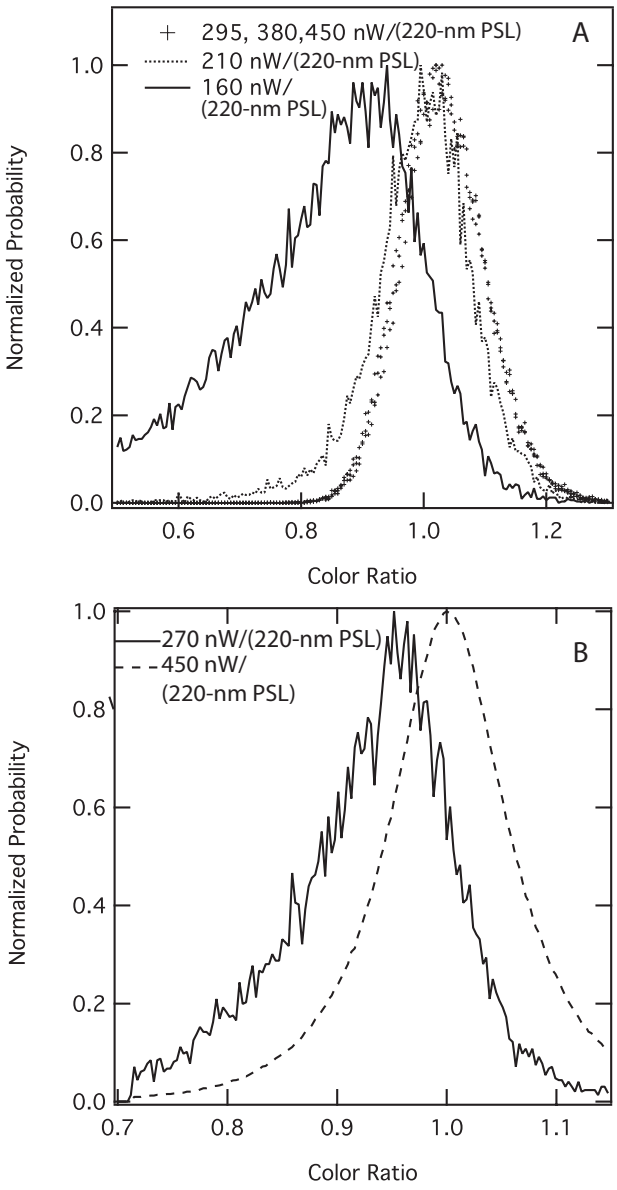

FIG. 7. Probability distributions of color ratios measured at different laser intensities. Ambient pressure was ∼1000 hPa. (a) Color ratios for 2-fg FSG particles coated with dioctyl sebacate to form a total particle mass of 4.5 fg. (b) color ratios for ambient rBC-containing aerosol measured during the Texas Air Quality study (Schwarz et al. 2008a) at pressures >900 hPa. Laser intensity is expressed in units of power (nW) detected due to scattering by 220-nm PSLs (see text). The relative gain in the red and blue channel detectors is chosen such that the color ratio associated with rBC is 1. The higher variability in the low intensity case in ambient aerosol is caused by the reduced statistical ensemble of rBC particles detected during the short time intervals of reduced laser intensity.

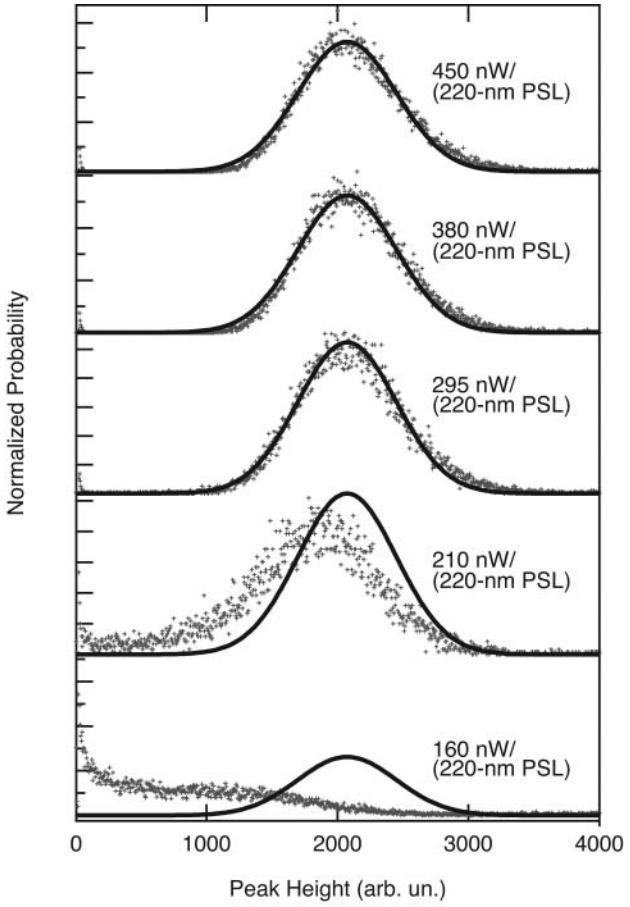

FIG. 8. Probability distributions of thermal radiation peak heights measured at different laser intensities for 2-fg FGS particles coated with dioctyl sebacate to form 4.5 fg total mass at 1000 hPa. Laser intensity is expressed in units of nW/(220-nm PSL), as described in the text. The histogram at the highest intensity was fit with a Gaussian function (black line), which is superposed on each of the lower intensity histograms as a guide to the eye. The histograms are normalized to the same number of particles.

increasing with laser intensity. In the case of the FGS data shown in Figure 7a, 295 nW/(220-nm PSL) would be identified as the TIPD for coated 2-fg rBC from FSG. The fact that different size rBC particles heat differently in the SP2 laser is a consequence of the relatively long interaction time between the laser and the particles. In the case of pulsed LII, with a pulse of extreme brevity, to first order the net energy absorbed by each particle is the same per unit rBC mass.

As an example of ambient data, Figure 7b shows color ratios measured as part of the Texas Air Quality Study (TexAQS) in 2006 at full laser intensity (approximately 450 nW/(220-nm PSL)) and at reduced laser intensity (for testing purposes, approximately 270 nW/(220-nm PSL)). The results for this accumulation-mode ambient aerosol show a loss of higher ratio values and a shift in the most probable color ratio to lower values, similar to the FGS results for a monodisperse aerosol. It is clear that 270 nW/(220-nm PSL) is below the TIPD for this ambient aerosol. The TexAQS results were obtained at ambient pressures >900 hPa.

Figure 8 and the previous discussion makes clear that even when the SP2 detects an rBC particle, insufficient laser intensity invalidates the rBC mass determination. Decreasing color ratio corresponding with reductions in laser intensity alert the user that the intensity is too low to bring the particles to vaporization for proper detection. Hence careful analysis of the ratio distribution and determination of the TIPD are powerful tools for estimating SP2 laser performance, even for ambient aerosols (i.e., aerosols with unknown rBC distributions). Practical determination of the TIPD is discussed in Section 6.2. In ambient airborne data sets from the NOAA SP2, the color ratio has been observed to be consistently monomodal, except for occasions of either insufficient laser intensity or cloud-induced contamination of the sampled aerosol (Murphy et al. 2004).

SP2 detection efficiency (SDE) results are shown in Figure 9 as a function of laser intensity for pairs of nascent and denuded FGS of the same rBC core mass. In each pair, the denuded mass represents the rBC-mass of the (internally mixed) nascent aerosol particles. The SDE values for both FGS types show consistent dependence on laser intensity. Starting from low efficiencies at low laser intensity, SDE increases with increasing laser intensity eventually reaching a plateau near unity. Particles with larger rBC cores tend to reach the plateau at laser intensities lower than for smaller rBC cores. This behavior is predicted from a very simple model of rBC heating in the laser beam, i.e., that the primary source of heat loss from a hot particle by convection depends on the surface area of the particle, while absorption of the laser light largely depends on its volume. Smaller (spherical) particles have a larger surface area/volume ratio and are therefore less likely to heat to vaporization in a given laser intensity than larger (spherical) particles. Particles with sufficient rBC mass to reach a plateau in Figure 9 are assumed to reach unity SDE. The variation of plateau values around unity is likely due to unsystematic errors (e.g., error in determination of the time offset between the CPC and the SP2 sampling or in the number fraction of primary mode particles determined from the SMPS). For the smallest rBC core size (0.19 fg) shown here, a plateau in SDE is not reached even at the highest laser intensity available, indicating that these particles are below the mass limit at which the SP2 will detect all rBC with reasonably high laser intensity (450 nW/(220-nm PSL)).

To first order one might expect that a non-absorbing coating on an rBC particle would decrease the likelihood that the particle would reach its vaporization temperature, as the coating would increase the particle surface area and, through its vaporization at relatively low temperature, provide an additional power loss term to an rBC core undergoing heating. The results shown in Figure 9 suggest this effect is not large as there is no obvious systematic differences in the SDE between the denuded and nascent aerosols at all laser intensities. Figure 10 shows SDE for a single rBC core mass of 1.9 fg associated with different thicknesses of coating material. Here, as in Figure 9, SDE increases with

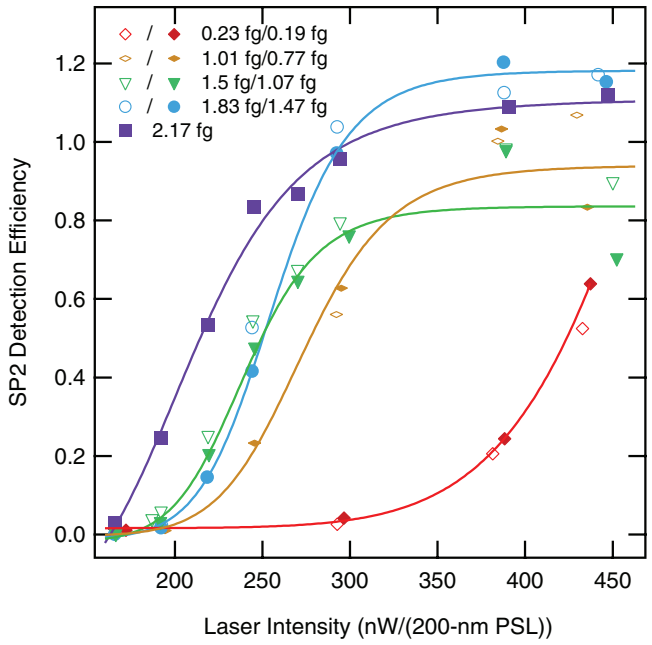

FIG. 9. SP2 detection efficiency (SPE) as a function of laser intensity for different FSG mass pairs of nascent and denuded particles measured at 1000 hPa. All the samples are from flames with equivalence ratio (φ) of 2.1. Particle masses are given in the legend as determined by the CPMA. Open symbols represent nascent soot particles, which have a non-refractory component. For each pair, the solid symbols represent the nascent aerosol denuded of non-refractory component. The denuded values are fit with Hill functions as a guide to the eye.

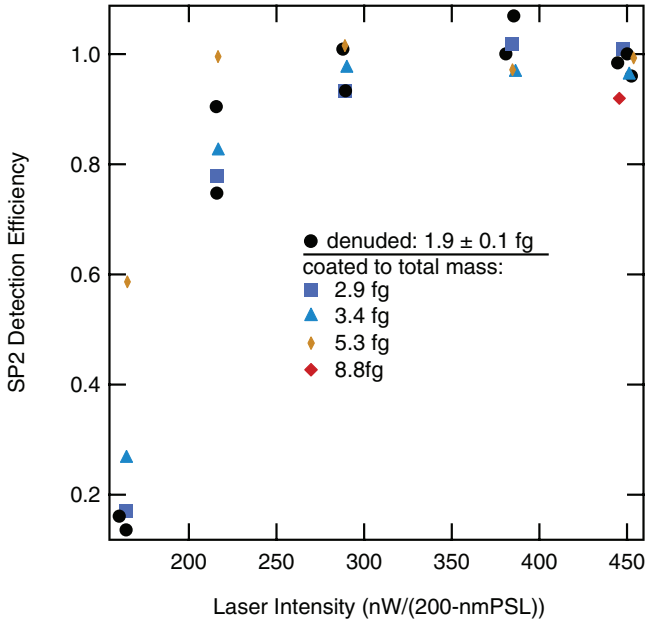

FIG. 10. Average SP2 detection efficiency for FSG generated with an equivalence ratio (φ) of 1.9, size selected with a DMA, and then coated with increasing thicknesses of sulfuric acid. The total-particle masses of the denuded rBC-core particles and coated particles as noted in the legend were determined with the CPMA. The denuded core mass was 1.9 ± 0.1 fg. Particles were sampled at 1000 hPa.

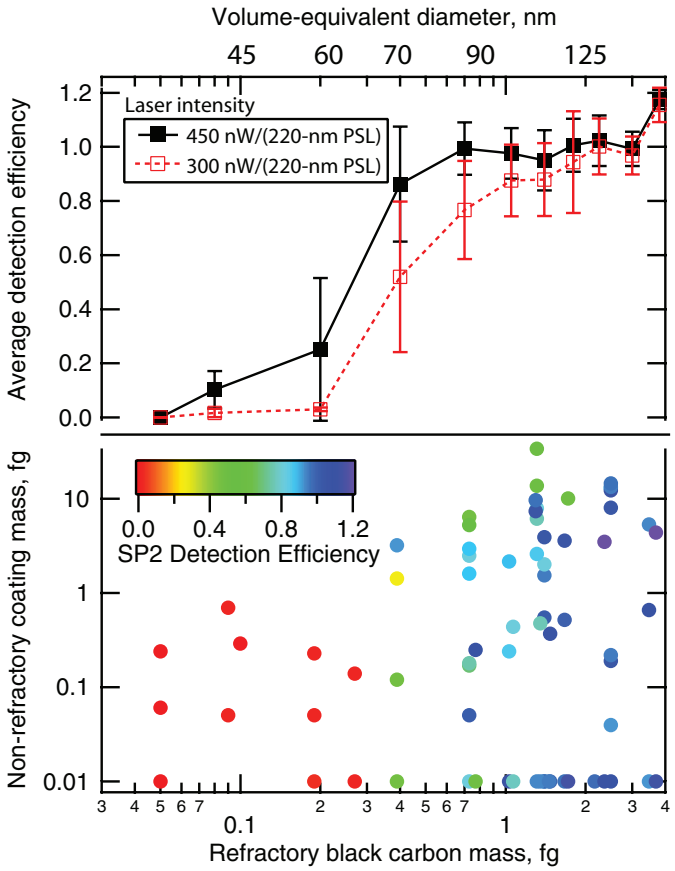

FIG. 11. Dependence of SP2 detection efficiency (SDE) on rBC-core mass, coating mass, and laser power measured at 1000 hPa for flame-generated soot. Bottom: SDE as a function of non-refractory coatings mass and rBC mass. Data points represent SDE for the experiments in which the denuded rBC-core mass (horizontal axis) was determined with the centrifugal particle mass analyzer (CPMA). The non-refractory coating mass (vertical axis) was determined by subtracting the denuded mass from the total particle mass as measured with the CPMA. Non-refractory mass was given a minimum value of 0.01 fg to allow plotting on a logarithmic scale. Points are colored by SP2 detection efficiency as shown in the legend. Top: The average detection efficiencies in each rBC mass-bin for each laser intensity shown in the legend. Whiskers represent the standard deviation of the values in each mass bin. The top axis shows volume-equivalent diameter (assuming 2 g/cc void-free density for rBC) that corresponds to denuded rBC-core mass on the bottom horizontal scale.

laser intensity up to a plateau indicating unity SDE. Coatings up to ~3.5 times the mass of the original rBC core do not affect SDE for this rBC mass. Multiple measurements of the denuded material are included in the figure to show the repeatability of the measurements.

The effect of wider ranges of internally mixed non-refractory mass and rBC-core mass on SDE are explored in Figure 11. rBC particles of a given mass were sampled by the SP2 in both nascent and denuded states with a wide range of additional coating mass of both sulfuric acid and DOS. The SDE for each aerosol type was recorded as the plateau value at the higher range of laser intensity as in Figures 9 and 10. If the plateau was not reached, then the value at the highest laser intensity

was used. For rBC cores more massive than 0.7-fg, SDE at high laser intensity was excellent (Figure 11 top panel, black curve)—averaging of 0.99 with a standard deviation of 10%. In contrast, for rBC cores below 0.3-fg, SDE averages 0.14 with a standard deviation of 10%. The limited measurements at ∼0.4-fg rBC cores show an average SDE of 0.86 with a standard deviation of 22%. Based on extensive measurements with laboratory rBC materials of masses >4 fg, we are confident that SP2 detection efficiency is 1 for larger rBC masses (up to at least 300 fg) with the laser intensities shown in Figure 11.

We identify the SP2 mass detection limit at a given laser intensity as the minimum rBC particle mass that provides an SDE within 10% of unity when measured at sea level — i.e., at rBC masses below this value SP2 counting of particle number is a lower bound. Thus, based on Figure 11, a conservative estimate of the lower mass detection limit of the SP2 with reasonable laser intensity (i.e., the highest tested here, 450 nW/(220-nm PSL)) is of 0.7 fg-rBC. This corresponds to 90 nm VED (with 2 g/cc void-free density).

Also plotted in Figure 11 (top panel, red curve) is the average SDE measured at a laser intensity of 300 nW/(220-nm PSL). This intensity is identified as the minimum intensity required to assess rBC mass loading in the accumulation mode in the ambient atmosphere at ∼1000 hPa pressure. At 300 nW/(220-nm PSL) laser intensity, average SDE is uniformly lower than at the higher laser intensity and yields better than 50% detection only for rBC masses of ∼0.5 fg and above. However, for rBC particles of mass between 1 and 2 fg, SDE sharply improves from 80% to unity. As 90% of rBC aerosol mass in the ambient atmosphere is typically associated with rBC larger than 1 fg (∼90 nm VED, Schwarz et al. 2008b), a conservative upper bound of errors in integrating typical rBC accumulation mode mass at this laser intensity is 20%. 300 nW/(220-nm PSL) is not sufficient for robust detection of rBC number at rBC masses below 2 fg at ∼1000 hPa pressure.

The results in Figures 7–11 lead to the question of whether SP2 detection of small rBC particles (i.e., below 0.7 fg) can be improved by increasing laser intensity beyond the highest value reported here. Referring again to a simple equilibrium model in which rBC absorption from the laser scales as spherical-particle volume, and convective heat loss to surrounding air scales as spherical-particle surface area, laser power is expected to have a dramatic impact on the minimum rBC core mass detectable in a single particle. In this model one would expect a doubling of laser intensity to lead to a halving of the minimum diameter of spherical particles that are brought to their vaporization temperature with an SDE of unity. However, as ambient rBC (and FGS) is formed of agglomerations of small spherules this extrapolation is likely not fully valid. The largest particles tested for which SDE was considered very low had rBC mass of 0.27 fg, with SDE peaking at ∼6% at the highest laser intensity tested. The dependence of SDE with laser power as shown in Figure 9 suggests that, at a minimum, a laser intensity of ∼600 nW/(220nm-PSL) would be required to reach a detection plateau for 0.27-fg rBC particles. Unfortunately laser intensities of 600 nW/(220-nm PSL) are currently not routinely achieved with typical SP2 configurations. It is reasonable to conjecture that as ambient pressure decreases (e.g., at high altitude in airborne measurements) the laser intensity required for good detection may also decrease due to the reduced power loss of hot rBC particles via convection. Unfortunately our previous tests of the pressure dependence of SP2 detection of rBC did not include evaluation of detection efficiency (Schwarz et al. 2006).

6.2. Laser Intensity Diagnostic Using Color Ratio Determinations

A method to determine absolute SP2 laser intensity based on light scattering from PSLs was described in Section 2.3. That method, although both useful and straightforward to carry out with other SP2 units, requires (as described) detailed knowledge of the APD and detection electronics of the SP2 to allow connection to the laser intensities cited in this paper. Here we present a complementary method to determine laser performance and absolute intensity without direct quantitative knowledge of the intensity. The method offers several benefits although it is not as straightforward as a PSL calibration. First, the method is independent of the detector setup and electronics. Second, it does not require sampling of a standard aerosol. Third, it does not depend on any proxy rBC material. We recommend performing this type of assessment routinely in laboratory and ambient measurements to provide an additional safeguard against SP2 operation with laser intensity insufficient for accurate rBC determinations.

This complementary method of evaluating laser performance is based on recognizing that the mere ability to measure the threshold intensity for proper detection (TIPD, as discussed in Section 6.1) implies sufficient laser intensity is available to properly detect the rBC used in the TIPD evaluation, and any of the same material of larger mass. Additionally, we have found that the TIPD determined for ambient rBC at sea level is a robust and absolute laser intensity reference that we have measured in units of nW/(220-nm PSL) (see below).

The TIPD is a robust reference for laser intensity for a particular rBC mass and material because it does not change with SP2 detection parameters other than operating pressure. For example, if the absolute and/or relative gains of the blue and red channel detectors are changed, determination of the TIPD is not affected. If the laser is not intense enough, at its most powerful, to bring all rBC in the mass range of interest to their vaporization temperatures, then it will not be possible to identify the TIPD, and the robust detection of rBC will not be assured. We conjecture that TIPD will weakly increase with increasing atmospheric pressure.

Section 6.1 describes the determination of the TIPD for laboratory FGS aerosol. The TIPD also can be identified from measurements of ambient polydisperse rBC aerosol. We have performed seven measurements of the TIPD near sea level in

diverse locations of the world (Alaska, Hawaii, the Cook Islands, New Zealand, and the Solomon Islands) over a three-week period. Approximately 10,000 ambient rBC particle events were recorded at each of ten laser intensities, from the highest available to an intensity that was obviously below the TIPD. We then determined the average color ratio associated with particles of refractory carbon mass in the range 1–3 fg (as determined by the SP2 measurement by assuming accurate detection). From the expected plateau dependence of color ratio on laser intensity, the TIPD was identified as the laser intensity at which the average color ratio fell to 98% of the plateau value for each set. We assume that differences in SP2 color maps will not be large enough to substantially change this determination. To determine the stability of this measurement, we normalized the plateau color ratio associated with each set of measurements to a value of 1, and compared the color ratios measured at fixed pump laser currents below that necessary to achieve the plateau value. They were stable to a fraction of a percent. The absolute range of laser intensity identified as the TIPD in this manner over the seven measurements was better than 20%, while the standard deviation of laser intensity values was better than 10%. This stability justifies using the TIPD for ambient rBC in this mass range at sea level as an absolute reference laser intensity. In terms of the intensity determined through the PSL measurement in the laboratory, the average sea level TIPD for ambient rBC in the mass range 1–3 fg was 500 ± 40 nW/(220-nm PSL). This value does not have an exact corollary to the intensities previously associated with the laboratory determinations of SDE, because it is not based on number-detection efficiency like the SDE. Nevertheless, it is possible to casually compare them: the ambient TIPD determination just described may be considered the minimum intensity to properly detect 1 fg ambient rBC particles. Thus, we would expect approximate agreement with the intensity of 450 nW/(220-nmPSL) identified in Section 6.1 as allowing high SPE of FGS down to 0.7 fg rBC at sea level. Clearly the two values, both of which may be interpreted as lower limits for detection of rBC around 1 fg are similar.

The variability in ambient color ratio measurements from day-to-day is large enough that for each daily set of measurements the plateau ratio must be determined independently. The NOAA SP2 software allows automatic scanning of laser intensity at regular intervals. This type of automation eases the process of recording data for determination of the TIPD. A new version of SP2 software that includes similar capabilities will soon available from the manufacturer.

As the TIPD is lower for more massive rBC particles its determination for the smallest rBC particles in a sample imply satisfactory laser intensity available for detection of larger particles. In the case of the ambient data described above, this implies that the TIPD determined for 1–3 fg rBC is sufficient for detection of typical accumulation mode rBC mass distributions (1–300 fg). Sufficient laser intensity for proper rBC detection is any value at or higher than the TIPD. As the TIPD is lower for more massive rBC particles, SP2s that cannot reach above 500 nW/(220-nm PSL) laser intensity (in order to use the ambient rBC TIPD reference described above) may at least identify an absolute reference at larger sizes by increasing integration time (which tend to lower number concentration in the ambient).

6.3. Dependence of rBC Thermal Radiation Signal Duration on Laser Intensity

The duration of an rBC particle's thermal radiation signal depends on laser intensity and air pressure due to the role of convection in drawing power from hot particles, while the peak signal does not. Thus, the time-integrated thermal emission signal is not generally a robust measure of rBC mass, everything else considered equal. Here we discuss the mechanisms affecting the integrated signal.

Even at a laser intensity that brings every rBC particle present in the aerosol jet fully to its vaporization temperature, there are portions of the laser beam traversed by each particle — on entry to and possibly on exit from the center of the Gaussian beam — in which the particles are not held at their vaporization temperatures. Absorbed laser power beyond that necessary to hold the rBC material at its vaporization temperature (balanced primarily by convective loss to the surrounding air) causes the phase change of the solid material to a vaporous state. Thus, as laser intensity is increased beyond the threshold to reach vaporization, the rate at which a solid rBC particle vaporizes will increase, and the size of the laser region intense enough to keep an rBC particle at vaporization also increases. Hence the integrated thermal radiation signal associated with rBC depends on laser intensity and on the size of the particle. For larger particles, which tend to have higher rates of vaporization, the integrated signal decreases with laser intensity. For smaller particles, which are only kept at vaporization temperatures in the most intense portions of the laser, increases in intensity increase the integrated signal.

Figure 12 shows SP2 data for two different size rBC particles measured over a range of laser intensities: a large 26-fg uncoated fullerene soot particle and a smaller 2 fg FGS particle coated with dioctyl sebacate to a total mass of 4.5 fg. As expected, the modal peak height associated with the particles is independent of laser intensity above a threshold close to 350 nW/(220-nm PSL), indicating that they are all brought to their vaporization temperatures at some point in the laser beam (bottom panel of Figure 12).

The time that the visible emissions were above baseline noise are shown for the two particle sizes in the top panel of Figure 12. As expected, the results show that the duration decreases with increasing laser intensity for the large rBC particle. In contrast, emissions from the small rBC particle are extended with increasing intensity. Thus, the length of time that the visible light signal persists depends on laser intensity, supporting the statement that peak height is a more robust measure of BC mass than the integral of the thermal emission signal.

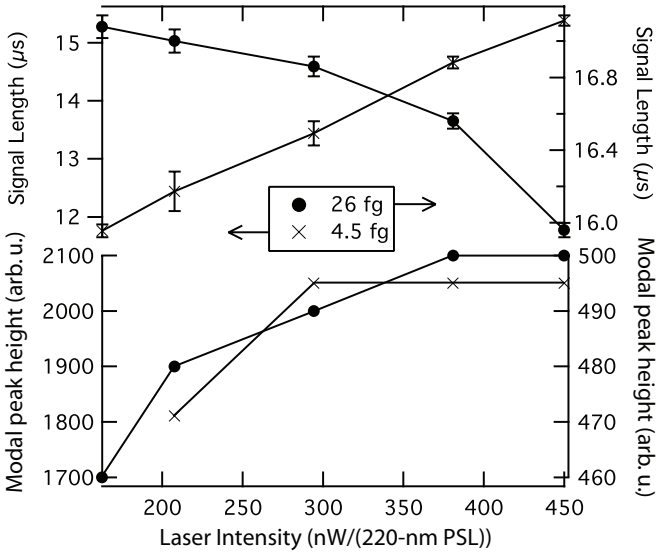

FIG. 12. Dependence of modal peak height and signal length as a function of laser intensity for the thermal emission from rBC particles. Values associated with small, 2 fg FGS particles coated with dioctyl sebacate to form 4.5 fg total mass are shown on the left axes. Values associated with large 26 fg fullerene particles are shown on the right axes. Top: Length of time that the blue channel signal associated with an rBC particle persisted above background noise, plotted as a function of laser intensity. Bottom: the modal peak heights associated with both particle sizes. The arbitrary units are not the same between the left-hand (4.5 fg) and right-hand (26 fg) axes. Measurements were made at 1000 hPa.

7. CONCLUSION AND RECOMMENDATIONS

The dependence of SP2 number-based detection efficiency (SDE) of particles containing rBC was explored as a function of rBC mass, additional internally mixed mass, and laser intensity using flame-generated soot (FGS). The results of this study, which are generally applicable to all SP2 instruments operating with a stable Gaussian laser beam at ambient pressures near sea level, identify: (a) a minimum laser intensity for accurate detection of typical ambient rBC mass loadings in the accumulation mode; (b) the lower detection limit of rBC-per-particle that ensures counting of rBC with near-unity efficiency with a laser intensity of 450 nW/(220-nm PSL); and (c) methods for identification of sufficient laser intensity for reliable rBC mass determination based on PSL sampling and on the analysis of rBC color ratios.

A method to measure the absolute SP2 laser intensity was described based on using PSLs to scatter a known fraction of the circulating laser intensity to the scatter detector of the SP2. Here 220 nm PSLs were used as the calibration standard; at the highest laser intensity tested here (1.7×10^5 W/cm^2) these particles scattered 450 nW onto the scatter detector from the center of the laser beam. This method requires that the SP2 be operated at stable temperature near 23°C, or that the temperature dependence of the scatter APD be independently quantified.

Measured low color temperatures of rBC particles serves as a flag to the SP2 operator that laser intensity is insufficient for both correct rBC mass determination and near-unity detection efficiency of small particle number in the accumulation mode. Shifts of color temperature to low values have been observed for both test aerosol and ambient rBC when laser intensity was reduced below a threshold value. This threshold, which we identify as the "threshold intensity for proper detection" (TIPD), is a function of particle mass, composition, morphology, and optical properties, as well as air pressure and composition, and can be used as an absolute reference laser intensity. For ambient sea level rBC in the mass range 1–3 fg, we have found that the TIPD corresponds to an absolute intensity of 500 ± 40 nW/(220-nm PSL).

A minimum laser intensity required to quantify rBC mass loadings in typical ambient conditions is found to be 300 nW/(200-nm PSL). At this intensity, the error due to undetected rBC in the mass-range of 1–300 fg (∼90 – 650 nm VED) detection is within 20% for a typical ambient rBC size distribution. This mass range typically contains ∼90% of the total rBC mass in the ambient accumulation mode. This intensity is not sufficient to determine rBC number for rBC masses below 2 fg at 1000 hPa pressure.

A conservative lower limit of denuded rBC particle mass for consistent, near-unity number-detection efficiency with the SP2 at sea level pressure and at the highest laser intensity available during testing (450 nW/(220-nm PSL)) has been identified as 0.7-fg rBC. This corresponds to a volume-equivalent diameter (VED) of 90 nm with an assumed density of 2 g/cm^3 for pure void-free rBC material. It is clear that below 0.4 fg rBC (i.e., 75-nm VED) SP2 detection efficiency falls sharply off at this laser intensity. At lower laser intensities the lower-detection limit of the SP2 increases. We are not confident that operation with laser intensities of higher - but demonstrably achievable - values will lower the lower detection limit enough to allow measurement of total rBC number in aged air masses or fresh emissions.

The following guidelines have been adopted for operation of the NOAA SP2, and are recommended to the wider SP2 community.

1. At regular intervals assess that the laser power is sufficient by performing a PSL calibration. This calibration is temperature dependent. Alternatively or additionally, examine the color ratio distribution dependence on laser intensity to determine the TIPD and verify sufficient intensity for proper detection.
2. Adopt a minimum laser intensity of 450 nW/(220-nm PSL) under non-exceptional conditions to ensure near-unity detection efficiency of rBC number down to masses of 0.7 fg at sea level. Maintaining laser intensity above 300 nW/(220-nm PSL) will ensure a robust (within 20%) measure of the accumulation mode rBC mass in the range 1–300 fg. Alternatively or additionally, determine that the laser intensity is above the TIPD for 1–3 fg rBC particles.
3. Use the peak height of thermal emissions as a measure proportional to rBC mass rather than the integrated thermal emission signal.
4. Set the gain of both red and blue channel detectors within the range 0.048–0.06 V/fg-rBC to optimize rBC mass detection

in typical ambient conditions and allow color-ratio determination for all particles. With this gain, the minimum rBC mass detectable with a reasonable choice of trigger level is ∼1 fg (corresponding to ∼100 nm VED), and the coverage of the rBC mass in typical ambient size ranges is optimized.

The results presented here bolster confidence in SP2 detection of accumulation mode rBC mass, which is a primary quantity of interest for determining rBC's direct radiative impact because this mode generally contains the most of the available mass in ambient samples observed away from available rBC sources. Accumulation-mode mass detection can be reliably achieved with moderate laser intensity. Excellent, near-unity detection efficiencies for particles with at least 0.7 rBC fg mass have been demonstrated.

GLOSSARY OF ABBREVIATIONS

APD	Avalanche photodetector
PSL	Polystyrene latex sphere
CPC	Condensation particle counter
CPMA	Coullette centrifugal particle mass analyzer
FGS	Flame-generated soot
PMT	Photomultiplier tube detector
rBC	Refractory black carbon
SDE	SP2 detection efficiency
SMPS	Scanning mobility particle sizer
TIPD	Threshold intensity for proper detection
VED	Volume equivalent diameter, assuming 2 g/cc density

REFERENCES

Andreae, M. O., and Gelenscér, A. (2006). Black or brown carbon? The nature of light-absorbing carbonaceous aerosols. *Atmos. Chem. Phys.* 6, 3131–3148.

Cross, E. S., Onasch, T. B., Ahern, A., Wrobel, W., Slowik, J. G., Olfert, J., Lack, D. A., Massoli, P., Cappa, C. D., Schwarz, J. P., Spackman, J. R., Fahey, D. W., Sedlacek, A., Trimborn, A., Jayne, J. T., Freedman, A., Williams, L. R., Ng, N. L., Mazzoleni, C., Dubey, M., Brem, B., Kok, G., Subramanian, R., Freitag, S., Clarke, A., Thornhill, D., Marr, L., Kolb, C. E., Warsnop, D. R., and Davidovits, P. (2010). Soot Particle Studies—Instrument Inter—Comparison—Project Overview. *Aero. Sci. Technol*. 44:592–611.

Flanner, M. G., Zender, C. S., Randerson, J.T., and Rasch, P. J. (2007). Present-day climate forcing and response from black carbon in snow. *J. Geophys. Res. 112,* D11202, doi:10.1029/2006JD008003.

Forster, P., Ramaswamy, V., Artaxo, P., Berntsen, T., Betts, R., Fahey, D. W., Haywood, J., Lean, J., Lowe, D. C., Myhre, G., Nhanha, J., Prinn, R., Raga, G., Schulz, M., and Van Dorland, R. (2007). Changes in Atmospheric Constituents and in Radiative Forcing. In: *Climate Change 2007: The Physical Science Basis. Contribution of Working Group I to the Fourth Assessment Report of the Intergovernmental Panel on Climate Change.* Solomon, S., D. Qin, M. Manning, Z. Chen, M. Marquis, K.B. Averyt, M.Tignor and H.L. Miller (eds.). Cambridge University Press, Cambridge, United Kingdom and New York, NY, USA.

Gao R. S, Schwarz, J. P., Kelly, K. K., Fahey, D. W., Watts, L. A., Thompson, T. L., Spackman, J. R., Slowik, J. G., Cross, E. S., Han, J.-H., Davidovits, P., Onasch, T. B., and Worsnop, D. R. (2007). A novel method for estimating light-scattering properties of soot aerosols using a modified single-particle soot photometer. *Aerosol Sci. Technol. 41,* doi:10.1080/02786820601118398.

Lohmann, U., and Feichter, J. (2001). Can the direct and semi-direct aerosol effect compete with the indirect effect on a global scale? *Geophys. Res. Lett.* 28:159.

Moteki, N., and Y. Kondo (2007). Effects of mixing state on black carbon measurements by laser-induced incandescence. *Aerosol Sci. Technol.* 41:398–417.

Moteki, N., and Kondo, Y. (2010). Dependence of laser-induced incandescence on physical properties of black carbon aerosols: measurements and theoretical interpretation. *Aerosol Sci. Technol*. 44:663–675.

Murphy, D. M., Cziczo, D. J., Hudson, P. K., Thomson, D. S., Wilson, J. C., Kojima, T., and Buseck, P. R. (2004). Particle generation and resuspension in aircraft inlets when flying in clouds. *Aerosol Sci. Technol*. 38: 400–408.

Olfert, J. S., and Collings, N. (2005). New method for particle mass classification — The Couette centrifugal particle mass analyzer. *J. Aerosol Sci.* 36, 1338–1352.

Olfert, J. S., Reavell, K. StJ., Rushton, M. G., & Collings, N. (2006). The experimental transfer function of the Couette centrifugal particle mass analyzer. *J. Aerosol Sci.* 37:1840–1852.

Petzold, A., and Schröder, F. P. (1998). Jet engine exhaust aerosol characterization. *Aerosol Sci. Technol. 28*:62–67.

Pierce, J. R., Chen, K., and Adams, P. J. (2007). Contribution of primary carbonaceous aerosol to cloud condensation nuclei: processes and uncertainties evaluated with a global aerosol microphysics model. *Atmos. Chem. Phys. 7*:5477–5466.

Pöschl, U. (2003). Aerosol particle analysis: challenges and progress. *Anal. Bioanal. Chem.* 375:30–32.

Schnaiter, M., Linke, C., Möhler, O., Naumann, K.-H., Saathoff, H., Wagner, R., Schurath, U., and Wehner, B. (2005). Absorption amplification of black carbon internally mixed with secondary organic aerosol. *J. Geophys. Res.*, 110, D19204, doi:10.1029/2005JD 006046.

Schulz, C., Kock, B. F., Hofmann, M., Michelsen, H., Will, S., Bougie, B., Suntz, R., and Smallwood, G. (2006). Laser-induced incandescence: recent trends and current questions. *Applied Physics B.,* Doi: 10.1007/s00340–006–2260–8.

Schwarz, J. P., R. S. Gao, D. W. Fahey, D. S. Thomson, L. A. Watts, J. C. Wilson, J. M. Reeves, M. Darbeheshti, D. G. Baumgardner, G. L. Kok, S. H. Chung, M. Schulz, J. Hendricks, A. Lauer, B. Kaercher, J. G. Slowik, K. H. Rosenlof, T. L. Thompson, A. O. Langford, M. Loewenstein, and K. C. Aikin (2006). Single-particle measurements of midlatitude black carbon and light scattering aerosols from the boundary layer to the lower stratosphere. *J. Geophys. Res.* Doi:10.1029/2006JD 007076.

Schwarz, J. P., Gao, R. S., Spackman, J. R., Watts, L. A., Thomson, D. S., Fahey, D. W., Ryerson, T., Peischel, J., Holloway, J., Trainer, M., Frost, G., Baynard, T., deGouw, J. A., Croon, K., and Del Negro, L. (2008a). Measurement of the mixing state, mass, and optical size of individual black carbon particles in urban and biomass burning emissions. *Geophys. Res. Lett.*, doi:10.1029/2008GL033968.

Schwarz, J. P., J. R. Spackman, D. W. Fahey, R. S. Gao, U. Lohmann, P. Stier, L. A. Watts, D. S. Thomson, D. A. Lack, L. Pfister, M. J. Mahoney, D. Baumgardner, J. C. Wilson, and Reeves, J. M. (2008b). Coatings and their enhancement of black–carbon light absorption in the tropical atmosphere. *J. Geophys. Res.,* doi:10.1029/2007JD 009042.

Shiraiwa, M., Y. Kondo, N. Moteki, N. Takegawa, L. K. Sahu, A. Takami, S. Hatakeyama, S. Yonemura, and D. R. Blake (2008). Radiative impact of mixing state of black carbon aerosol in Asian outflow. *J. Geophys. Res.*, 113, D24210, doi:10.1029/2008JD010546.

Slowik, J., Stainken, K., Davidovits, P., Williams, L. R., Jayne, J. T., Kolb, C. E., Worsnop, D. R., Rudich, Y., DeCarlo, P., and Jimenez, J. L. (2004). Particle Morphology and Density Characterization by Combined Mobility and Aerodynamic Diameter

Measurements. Part 2: Application to Combustion Generated Soot Particles as a Function of Fuel Equivalence Ratio. *Aerosol Sci. Technol.* 38: 1206–1222.

Slowik, J.G., Cross, E.S., Han, J.-H., Davidovits, P., Onasch, T.B., Jayne, J.T., Williams, L.R., Canagaratna, M.R., Worsnop, D.R. Chakrabarty, R.K., Moosmüller, H., Arnott, W.P., Schwarz, J.P., Gao, Ru-Shan, Fahey, David W., Kok, G.L., Petzold, A. (2007). An Inter-Comparison of Instruments Measuring Black Carbon Content of Soot Particles. *Aerosol Sci. Technol.* 41: 295–314.

Stephens, M., Turner, N., and Sandberg, J. (2003). Particle Identification by Laser–Induced Incandescence in a Solid-State Laser Cavity. *Appl. Opt.* 42:3726–3736.

Tripathi, S. N., Dey, S., Tare, V., and Satheesh, S. K. (2005). Aerosol Black Carbon Radiative Forcing at an Industrial City in Northern India. *Geophys. Rev. Lett.* 32:L08802.

Zuberi, B., Johnson, K. S., Aleks, G. K., Molina, L. T., Molina, M. J., and Laskin, A. (2005). Hydrophilic Properties of Aged Soot. *Geophys. Res. Lett.* 32:L01807.